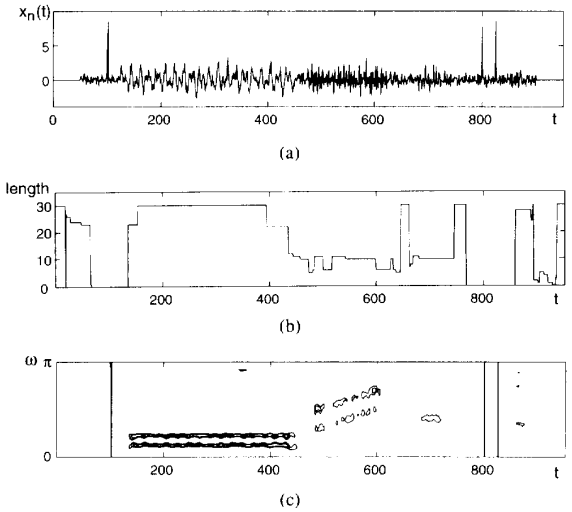

Fig. 5. (a) Synthetic signal shown in Fig. 1 corrupted by additive white Gaussian noise 5.3 dB below the signal. (SNR computed over the entire signal.) The optimal cone length in the noise-corrupted case is approximately the same as that shown in Fig. 3 (a), and the TFD shown in (c) is noise-corrupted, but recognizably the same as in Fig. 3 (b); the close impulses are still resolved, and the separation between the parallel sinusoids and chirps is clearly visible. Like Fig. 3, the TFD is computed with a length 64 FFT and an analytic signal.

else have varying frequency components that run nearly parallel in the time-frequency plane. In fact, we have had some success in analyzing signals that lack this simple character, but we note that the strength of the cone-kernel distribution is in analyzing components that lie along the τ axis of the ambiguity plane, e.g., sinusoids. While the CKD is a good general purpose distribution, it is important to keep in mind its inherent strengths and weaknesses, because any adaptive version will share those properties.

IV. Conclusions

This correspondence presents a technique for adaptively optimizing the performance of the cone-kernel distribution that offers high performance at a very modest computational cost. The algorithm requires the calculation of the optimal cone length at each time; this requires less computation than the FFT used in computing each time-slice, making the adaptation practically free when a dense sampling of the TFR is desired.

This single-parameter adaptive kernel TFR represents the "entry-level" of adaptive time-frequency analysis, offering performance similar to that of more sophisticated techniques, but at little cost to the user above that of a fixed-kernel representation. While more expensive algorithms can achieve higher performance with some signals, for many real signals we and others have found that this simple adaptation gives the best results of any TFD known to us.

References

[1] L. Cohen, "Time-frequency distributions—a review," *Proc. IEEE*, vol. 77, no. 7, pp. 941–981, July 1989.

[2] D. L. Jones and T. W. Parks, "A high resolution data-adaptive time-frequency representation," *IEEE Trans. Acoust., Speech, Signal Processing*, vol. 38, no. 12, pp. 2127–2135, Dec. 1990.

[3] R. G. Baraniuk and D. L. Jones, "A signal-dependent time-frequency representation: Optimal kernel design," *IEEE Trans. Signal Processing*, vol. 41, no. 4, pp. 1589–1602, Apr. 1993.

[4] ——, "Signal-dependent time-frequency analysis using a radially-Gaussian kernel," *Signal Processing*, vol. 32, no. 3, pp. 263–284, June 1993.

[5] J. W. Pitton, L. E. Atlas, and P. J. Loughlin, "Deconvolution for positive time-frequency distributions," in *Proc. 27th Asilomar Conf. Signals, Systems, Computers*, Nov. 1–3 1993, pp. 1450–1454.

[6] B. Ristic and B. Boashash, "Kernel design for time-frequency signal analysis using the Radon transform," *IEEE Trans. Signal Processing*, vol. 41, no. 5, pp. 1996–2008, May 1993.

[7] T. A. C. M. Claasen and W. F. G. Mecklenbräuker, "The Wigner distribution—A tool for time-frequency signal analysis—Part III: Relations with other time-frequency signal transformations," *Phillips J. Research*, vol. 35, no. 6, pp. 372–389, 1980.

[8] Y. Zhao, L. E. Atlas, and R. J. Marks, "The use of cone-shaped kernels for generalized time-frequency representations of nonstationary signals," *IEEE Trans. Acoust., Speech, Signal Processing*, vol. 38, no. 7, pp. 1084–1091, July 1990.

[9] P. J. Loughlin, J. W. Pitton, and L. E. Atlas, "Bilinear time-frequency representations: New insights and properties," *IEEE Trans. Signal Processing*, vol. 41, no. 2, pp. 750–767, Feb. 1993.

[10] S. Oh and R. J. Marks, "Some properties of the generalized time frequency representation with cone-shaped kernel," *IEEE Trans. Signal Processing*, vol. 40, no. 7, pp. 1735–1745, July 1992.

[11] P. Flandrin, "Some features of time-frequency representations of multi-component signals," in *Proc. IEEE ICASSP '84*, San Diego, CA, Mar. 1984.

[12] M. G. Amin, "Recursion in Wigner distribution," in *Advanced Algorithms and Architectures for Signal Processing III*, F. T. Luk, Ed., Proc. SPIE 975, 1988, pp. 221–231.

[13] M. Unser, "Recursion in short-time signal analysis," *Signal Processing*, vol. 5, no. 3, pp. 229–240, May 1983.

[14] M. G. Amin, "Computationally lag-invariant recursive spectrum estimators," *IEEE Trans. Signal Processing*, vol. 35, pp. 1713–1724, Dec. 1987.

[15] ——, "Order-recursive spectrum estimation," *Proc. IEEE*, vol. 76, no. 3, pp. 289–290, Mar. 1988.

[16] D. J. Borror, "Common bird songs (cassette)," New York: Dover Publications, Inc., 1984.

On the Local Frequency, Group Shift, and Cross-Terms in Some Multidimensional Time-Frequency Distributions: A Method for Multidimensional Time-Frequency Analysis

Srdjan Stanković, LJubiša Stanković and Zdravko Uskoković

***Abstract*— This correspondence presents an analysis of the representation of local frequency and group shift using multidimensional time-frequency distributions. In the second part of the correspondence, we extend the analysis to the multicomponent signals and cross-terms effects. On the basis of that analysis, an efficient method, derived from the analysis of the multidimensional Wigner distribution defined in the frequency domain, is proposed. This method provides some substantial advantages over the Wigner distribution: the well known cross-terms' effects are reduced or completely removed; the oversampling of signals is shown to be unnecessary; and the computation time can be significantly reduced, as well. The theory is illustrated by a two-dimensional numerical example.**

Manuscript received December 7, 1993; revised January 10, 1995. The associate editor coordinating the review of this paper and approving it for publication was Dr. Patrick Flandrin.

The authors are with Elektrotehnicki Fakultet, Cetinjski put b.b., 81000 Podgorica, Montenegro, Yugoslavia.

IEEE Log Number 9412002.

I. Introduction

One-dimensional time-frequency distributions (TFD) have been intensively studied during the last decade. We refer to review papers on the distributions for time-frequency analysis [1], [2]. Several results dealing with the multidimensional case are reported in [2].

It is desirable that a multidimensional time-frequency distribution (MTFD) of a signal $x(\vec{r})$ satisfies the following basic properties

$$\frac{1}{(2\pi)^n}\int_{R^n}\int_{R^n}\text{MTFD}(\vec{\omega},\vec{r})\,dV_{\vec{\omega}}dV_{\vec{r}} = E_x \tag{1}$$

$$\frac{1}{(2\pi)^n}\int_{R^n}\text{MTFD}(\vec{\omega},\vec{r})\,dV_{\vec{\omega}} = |x(\vec{r})|^2$$
$$\int_{R^n}\text{MTFD}(\vec{\omega},\vec{r})\,dV_{\vec{r}} = |X(\vec{\omega})|^2 \tag{2}$$

where E_x denotes the energy of $x(\vec{r})$; $X(\vec{\omega})$ is the n-dimensional Fourier transform of $x(\vec{r})$; and $dV_{\vec{\omega}}$ and $dV_{\vec{r}}$ are the n-dimensional differential elements of R^n. An infinite number of distributions satisfying (1) and (2) can be defined—the multidimensional extension of the Cohen class of distributions [1].

The previous relations do not tell anything about the local distribution of energy at a point $(\vec{\omega},\vec{r})$. In Section II we impose some more specific requirements than the ones defined by (1) and (2). Those requirements turn out to be very reasonable and meaningful for the analysis of some classes of signals, both monocomponent and multicomponent, as it will be shown in Sections II, III, and IV. This analysis is used to develop an efficient multidimensional time-frequency distribution, extending our previously defined one-dimensional method [4], [6]–[8].

II. Local Frequency Presentation

Consider an n-dimensional signal

$$x(\vec{r}) = g(\vec{r})e^{j\Phi(\vec{r})} \tag{3}$$

with $\vec{r} = (r_1, r_2, \cdots, r_n) \in R^n$ and $g(\vec{r})$ slow-varying n-dimensional function. The associated local frequency at a point is defined as $\vec{\omega} = \nabla\Phi(\vec{r})$, with $\vec{\omega} = (\omega_1, \omega_2, \cdots, \omega_n)$, while ∇ denotes the Hamiltonian operator. For this class of signals we will require that the ideal MTFD has the local power $|g(\vec{r})|^2$ concentrated at the local frequency

$$\text{IMTFD}(\vec{r},\vec{\omega}) = (2\pi)^n|g(\vec{r})|^2\delta[\vec{\omega} - \nabla\Phi(\vec{r})]. \tag{4}$$

This form has already been defined and used in the one-dimensional case [5], [7], [11]. We will now compare the commonly used TFD with the one defined by (4).

A. Multidimensional Short Time Fourier Transform

The short time Fourier transform (STFT) of the signal $x(\vec{r})$ is defined by

$$\text{STFT}(\vec{r},\vec{\omega}) = \int_{R^n} x(\vec{r}+\vec{v})w^*(\vec{v})e^{-j\vec{\omega}\vec{v}}dV_{\vec{v}} \tag{5}$$

where $w^*(\vec{r})$ denotes an n-dimensional, usually even real-valued, window function. It will be assumed that $w(\vec{r}) = 0$ holds outside the bounded n-dimensional region $D \subset R^n$.

Substituting signal (3) into (5) and expanding $\Phi(\vec{r}+\vec{v})$ into a Taylor series[1] around $\vec{r}$, we obtain

$$\text{STFT}(\vec{r},\vec{\omega}) = \frac{1}{(2\pi)^n}g(\vec{r})e^{j\Phi(\vec{r})} \times \delta[\vec{\omega} - \nabla\Phi(\vec{r})] *_{\vec{\omega}} W(\vec{\omega}) *_{\vec{\omega}} \text{FT}\left[e^{j\frac{(\vec{v}\nabla)^2}{2!}\Phi(\vec{r}_1)}\right] \tag{6}$$

where $*_{\vec{\omega}}$ denotes an n-dimensional convolution operator with respect to $\omega_1, \omega_2, \cdots, \omega_n$, and $g(\vec{r})$ is treated as a constant inside the window $w(\vec{r})$, i.e., $g(\vec{r}+\vec{v})w(\vec{v}) \cong g(\vec{r})w(\vec{v})$.

If the second and higher-order partial derivatives of $\Phi(\vec{r})$ may be neglected in (6), then the associated spectrogram (squared magnitude of the STFT) becomes

$$\text{SPEC}(\vec{r},\vec{\omega}) = |\text{STFT}(\vec{r},\vec{\omega})|^2 = |g(\vec{r})|^2W^2[\vec{\omega} - \nabla\Phi(\vec{r})]. \tag{7}$$

Observe that the spectrogram (7) exhibits all desirable properties of the ideal distribution (4), provided the behavior of $W^2(\vec{\omega})$ is close to $(2\pi)^n\delta(\vec{\omega})$. If, on the other hand, higher-order partial derivatives are not negligible, the spectrogram contains artifacts even for the ideal behavior of $W(\vec{\omega})$.

B. Multidimensional Wigner Distribution

Another distribution that is very commonly used in the time-frequency analysis is the pseudo-Wigner distribution (PWD), defined by

$$\text{PWD}(\vec{r},\vec{\omega}) = \int_{R^n} x(\vec{r}+\vec{v}/2)x^*(\vec{r}-\vec{v}/2)w_s(\vec{v})e^{-j\vec{\omega}\vec{v}}dV_{\vec{v}},$$
$$\text{with}\quad w_s(\vec{v}) = w(\vec{v}/2)w^*(-\vec{v}/2). \tag{8}$$

For signals (3), upon substitution in (8) and expansion of $\Phi(\vec{r}+\vec{v}/2)$ and $\Phi(\vec{r}-\vec{v}/2)$ into Taylor series, the following expression for the PWD is obtained

$$\text{PWD}(\vec{r},\vec{\omega}) = \frac{1}{(2\pi)^n}|g(\vec{r})|^2\delta[\vec{\omega} - \nabla\Phi(\vec{r})] *_{\vec{\omega}} W_s(\vec{\omega}) *_{\vec{\omega}} \times \text{FT}\left[e^{j\frac{[(\vec{v}/2)\nabla]^3}{3!}[\Phi(\vec{r}_1)+\Phi(\vec{r}_2)]}\right]. \tag{9}$$

The PWD provides an ideal time-frequency representation if the third- and higher order partial derivatives of $\Phi(\vec{r})$ are negligible. This is obviously a significant improvement over the STFT.

C. Cohen Class of Distributions

We have seen that the WD of a signal whose phase does not contain third and higher-order terms produces the ideal space-frequency representation. We may ask then, whether there exists another distribution from the Cohen class with the same ideal representation for the above shape of signals. The Cohen formula, defining the associated class of distributions for n-dimensional signals, is

$$\text{CD}(\vec{r},\vec{\omega}) = \frac{1}{(2\pi)^n}\int_{R^n}\int_{R^n}\int_{R^n} x(\vec{u}+\vec{v}/2)x^*(\vec{u}-\vec{v}/2) \times c(\vec{\theta},\vec{v})e^{-j\vec{\theta}\vec{r}-j\vec{\omega}\vec{v}+j\vec{\theta}\vec{u}}\,dV_{\vec{\theta}}\,dV_{\vec{v}}\,dV_{\vec{u}} \tag{10}$$

[1] Taylor series for an n-dimensional function is of the form

$$\Phi(\vec{r}+\vec{v}) = \sum_{i=0}^{m-1}\frac{(\vec{v}\nabla)^i}{i!}\Phi(\vec{r}) + \frac{(\vec{v}\nabla)^m}{m!}\Phi(\vec{r}_1)$$

with $\vec{r}_1 = \vec{r}+\vec{v}_1$, and $0 < v_{1h} < v_h$ for each $h = 1, 2, \cdots, n$.

with $\vec{u}, \vec{r}, \vec{\theta}, \vec{r}, \vec{\omega} \in R^n$, while $c(\vec{\theta}, \vec{v})$ represents so called kernel function for an n-dimensional case. Assume now that the phase function $\Phi(\vec{r})$ is quadratic, i.e., that it possesses the following property

$$\nabla^i \Phi(\vec{r}) = 0 \quad \text{for} \quad i \geq 3. \quad \text{i.e.} \quad \nabla\Phi(\vec{r}) = \vec{r}\mathbf{B} + \vec{d} \tag{11}$$

where $\mathbf{B} \in R^{n \times n}$ is a constant symmetric matrix, while $\vec{d}$ is a row vector.

Expanding the functions $\Phi(\vec{u} + \vec{v}/2)$ and $\Phi(\vec{u} - \vec{v}/2)$ into a Taylor series around $\vec{u}$, and taking into account (11), integration over $\vec{\theta}$ and $\vec{u}$ produces

$$\mathrm{CD}(\vec{r}, \vec{\omega}) = |g(\vec{r})|^2 \int_{R^n} c(-\vec{v}\mathbf{B}, \vec{v}) e^{-j[\vec{\omega} - (\vec{r}\mathbf{B} + \vec{d})]\vec{v}} dV_{\vec{v}}. \tag{12}$$

Equating the right-hand sides of (12) and (4) leads to the conclusion that the function $c(-\vec{v}\mathbf{B}, \vec{v})$ has to be equal to unity. For a given signal, it means that the kernel $c(\vec{\theta}, \vec{v})$ should be equal to unity on the n-dimensional subspace Π: $\vec{\theta} = -\vec{v}\mathbf{B}$ of the $(\vec{\theta}, \vec{v})$ space, while it may take any value outside Π. But if one wants to use the signal independent kernel (as it is done in this paper), then $c(\vec{\theta}, \vec{v}) = 1$ should hold for any $\mathbf{B}$, i.e. everywhere in $(\vec{\theta}, \vec{v})$ space. The distribution from the Cohen class, with the unity kernel, corresponds to the WD (for one-dimensional case see [6], [7], [11]).

The above analysis proves that out of all distributions from the Cohen class, the WD is the only one that produces the ideal representation of the signals with quadratic phase.

III. Analysis of Multidimensional Multicomponent Signals

Let us consider now an n-dimensional multicomponent signal given by

$$x(\vec{r}) = \sum_{i=1}^{p} g_i(\vec{r}) e^{j\Phi_i(\vec{r})} \tag{13}$$

where the functions $g_i(\vec{r})$, $i = 1, \cdots, p$, belong to the same class as $g(\vec{r})$ in (3).

In analogy with the previous considerations, the spectrogram for signal (13) may be shown to be

$$\mathrm{SPEC}(\vec{r}, \vec{\omega}) = \sum_{i=1}^{p} \sum_{k=1}^{p} g_i(\vec{r}) g_k(\vec{r}) e^{j[\Phi_i(\vec{r}) - \Phi_k(\vec{r})]} \times W[\vec{\omega} - \nabla\Phi_i(\vec{r})] W^*[\vec{\omega} - \nabla\Phi_k(\vec{r})] \tag{14}$$

where we have neglected the artifacts due to higher-order partial derivatives of $\Phi_i(\vec{r})$, $i = 1, 2, \cdots, p$, i.e. $\nabla\Phi_i(\vec{r})$ is treated as a constant vector inside $w(\vec{r})$.

Generally, the spectrogram contains the cross-terms, but they are absent, provided the condition

$$W[\vec{\omega} - \nabla\Phi_i(\vec{r})] W^*[\vec{\omega} - \nabla\Phi_k(\vec{r})] = 0 \text{ for any } \vec{\omega} \text{ and } i \neq k \text{ or } \|\nabla\Phi_i(\vec{r}) - \nabla\Phi_k(\vec{r})\| > W_i \tag{15}$$

is satisfied; $\|\cdot\|$ denotes an appropriately defined norm in R^n. This means that cross-terms do not appear if the n-dimensional distance between local frequencies is greater than the maximal width of the $W(\vec{\omega})$ along the direction $\vec{\ell} = \nabla\Phi_i(\vec{r}) - \nabla\Phi_k(\vec{r})$, connecting the i-th and k-th local frequency, Fig. 1. In that case

$$\mathrm{SPEC}(\vec{r}, \vec{\omega}) = \sum_{i=1}^{p} |g_i(\vec{r})|^2 W^2[\vec{\omega} - \nabla\Phi_i(\vec{r})]. \tag{16}$$

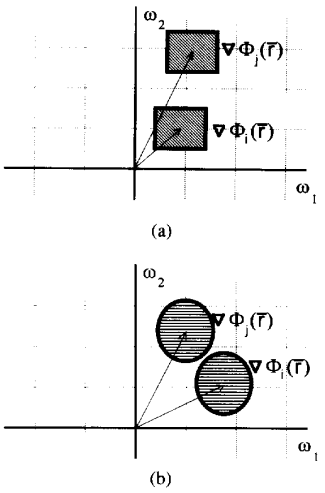

Fig. 1. Illustration of energy location in spectrograms without cross-terms: (a) separable and (b) nonseparable window $w(\vec{r})$.

Observe that the PWD, defined by (8), may be expressed as

$$\mathrm{PWD}(\vec{r}, \vec{\omega}) = \frac{1}{\pi^n} \int_{R^n} \mathrm{STFT}(\vec{r}, \vec{\omega} + \vec{\theta}) \mathrm{STFT}^*(\vec{r}, \vec{\omega} - \vec{\theta}) \, dV_{\vec{\theta}}. \tag{17}$$

Substituting expression (6) into (17), appropriately adjusted to account for the class of signals defined by (13) and neglecting the artifacts, we obtain

$$\mathrm{PWD}(\vec{r}, \vec{\omega}) = \frac{1}{\pi^n} \sum_{i=1}^{p} \sum_{k=1}^{p} g_i(\vec{r}) g_k(\vec{r}) e^{j[\Phi_i(\vec{r}) - \Phi_k(\vec{r})]} \times \int_{R^n} W[\vec{\omega} + \vec{\theta} - \nabla\Phi_i(\vec{r})] \times W^*[\vec{\omega} - \vec{\theta} - \nabla\Phi_k(\vec{r})] \, dV_{\vec{\theta}}. \tag{18}$$

We will now use the above expression to analyze cross-terms in the PWD for the n-dimensional multicomponent signals. The integrand in (18) is nonzero for

$$\vec{\omega} + \vec{\theta} - \nabla\Phi_i(\vec{r}) \in D_w \quad \text{and} \quad \vec{\omega} - \vec{\theta} - \nabla\Phi_k(\vec{r}) \in D_w \tag{19}$$

meaning that $\mathrm{PWD}(\vec{r}, \vec{\omega}) \neq 0$, for

$$\vec{\omega} \in D_\omega(i,k) : (\vec{\omega} - [\nabla\Phi_i(\vec{r}) + \nabla\Phi_k(\vec{r})]/2) \in D_w$$

and

$$\vec{\theta} \in D_\theta(i,k) : (\vec{\theta} - [\nabla\Phi_i(\vec{r}) - \nabla\Phi_k(\vec{r})]/2) \in D_w \tag{20}$$

where the Fourier transform $W(\vec{\omega})$ of $w(\vec{r})$ is assumed to be nonzero only inside a bounded region $D_w \subset R^n$, and D_w is convex and symmetric with respect to the origin (i.e. $w(\vec{r})$ is real).

This means that the auto-terms ($i = k$) are concentrated within the region centered at the local auto-frequencies of each component of signal (13), i.e., at $\vec{\omega}_i = \nabla\Phi_i(\vec{r})$, $i = 1, 2, \cdots, p$, while the cross-terms are centered between the corresponding auto-frequencies. Relation (20) also implies that, along the axes of the n-dimensional convolution $\vec{\theta}$, all auto-terms are concentrated at $\vec{\theta} = 0$ and its neighborhoods. The cross-terms are dislocated from the $\vec{\theta}$ origin. Having this in mind, we conclude that the cross-terms may be removed from the PWD of a multicomponent signal, and at the same time the integration over auto-terms performed, if the convolution

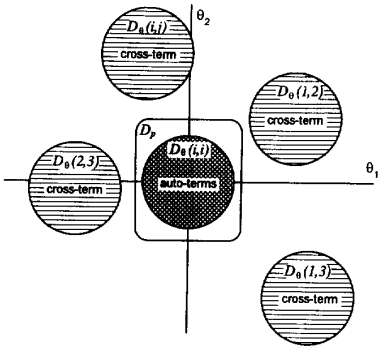

Fig. 2. Auto-terms, cross-terms, and window $P(\vec{\theta})$ support illustration in $\vec{\theta}$ space.

(17) is evaluated within an n-dimensional window function $P(\vec{\theta})$, in the following way

$$\text{MWD}(\vec{r},\vec{\omega}) = \frac{1}{\pi^n}\int_{R^n} P(\vec{\theta})\text{STFT}(\vec{r},\vec{\omega}+\vec{\theta}) \times \text{STFT}^*(\vec{r},\vec{\omega}-\vec{\theta})\,dV_{\vec{\theta}} \quad (21)$$

where the region of support D_p of the window function $P(\vec{\theta})$ must comply with the conditions defined in (20), i.e., $D_p \supset D_w \equiv D_\theta(i,i)$ and $D_p \bigcap D_\theta(i,k) = \emptyset$ for $i \neq k$, Fig. 2.

The distribution (21) is derived from the condition that its auto-terms are equal to the auto-terms in the WD. But, in contrast to the WD, this distribution is cross-terms free (under the described conditions). Thus, the obtained distribution is equal to the sum of the WD of the individual components. Note that the distribution (21) does not satisfy the marginal properties in the case of multicomponent signals. Many other distributions have been developed with the purpose of the cross-terms' reduction, [1], [12], [13], [16]. A detailed comparison of these distributions in the one-dimensional case may be found in [9].

Distribution (21), besides its efficiency in cross-terms removal and the preservation of the auto-terms presentation quality as in the WD, leads to a numerically more efficient method than the WD realization itself. This will be shown in Section VI (for one-dimensional case see [4], [6], [7]).

IV. Group Shift

If the signal $x(\vec{r})$ is nonzero-valued within the short intervals of the axes r_h, $h = 1, 2, \cdots, n$, then the Fourier transform of $x(\vec{r})$ is more convenient tool for the presented analysis. Let us consider the signal $x(\vec{r})$ whose Fourier transform $X(\vec{\omega})$ is of the form

$$X(\vec{\omega}) = R(\vec{\omega})e^{j\varphi(\vec{\omega})} \quad (22)$$

where $R(\vec{\omega})$ is an n-dimensional slow-varying function, i.e., it may be treated as a constant inside D_w. The group shift, a concept dual to the local frequency, is defined as $\vec{r}_g = -\nabla\varphi(\vec{\omega})$. The IMTFD for the signals of form (22) may be defined, in analogy with (4), as

$$\text{IMTFD}(\vec{r},\vec{\omega}) = |R(\vec{\omega})|^2\delta[\vec{r}+\nabla\varphi(\vec{\omega})]. \quad (23)$$

A definition of the STFT in the frequency domain is

$$\text{STFT}(\vec{r},\vec{\omega}) = \frac{e^{j\vec{\omega}\vec{r}}}{(2\pi)^n}\int_{R^n} X(\vec{\theta}+\vec{\omega})W^*(\vec{\theta})e^{j\vec{\theta}\vec{r}}dV_{\vec{\theta}} \quad (24)$$

while the PWD in an n-dimensional frequency domain is

$$\text{PWD}(\vec{r},\vec{\omega}) = \frac{1}{(2\pi)^{2n}}\int_{R^n} X(\vec{\omega}+\vec{\theta}/2,\vec{r})X^*(\vec{\omega}-\vec{\theta}/2,\vec{r}) \times e^{j\vec{\theta}\vec{r}}dV_{\vec{\theta}} *_{\vec{\omega}} W_s(\vec{\omega}). \quad (25)$$

Thus, we may easily conclude that all the earlier derived properties (6), (7), (9), are also valid in the dual sense.

V. Analysis of the Aliasing Effects

The aliasing effects are interesting in the WD [2]. Because of the quadratic nature of the WD, its direct realization requires the signal to be oversampled by a factor of two, with respect to the sampling interval defined in the sampling theorem. The analytic part of the signal has been commonly used as a way to avoid aliasing (or oversampling) in the WD. Recently, some other techniques for this purpose have been derived (for a reference list, see [14]). Here, we will show that the aliasing components appearing in the WD may be eliminated, using the distribution (21), in the same manner as the cross terms.

Consider multidimensional signal $x_d(\vec{r})$, obtained by sampling a continuous signal $x(\vec{r})$.

$$x_d(\vec{r}) = \sum_{k_1=-\infty}^{\infty}\cdots\sum_{k_n=-\infty}^{\infty} T_1\cdots T_n x(k_1T_1,\cdots,k_nT_n) \times \delta(r_1-k_1T_1,\cdots,r_n-k_nT_n) \quad (26)$$

where T_h represents the sampling period along the h-th axis, $h = 1, 2, \cdots, n$.

The Fourier transform of $x_d(\vec{r})$ is a periodic function along all frequency axes, with the corresponding periods $\omega_{ph} = 2\pi/T_h$, and has the form

$$X_d(\vec{\omega}) = \sum_{R^k} X[(\vec{\omega}+\vec{\omega}_{pk}] \quad (27)$$

with $\vec{\omega}_{pk} = (k_1\omega_{p1}, k_2\omega_{p2}, \cdots, k_n\omega_{pn})$, while the sum over R^k represents an n-dimensional sum over the coordinates of the vector $\vec{k} = (k_1, k_2, \cdots, k_n)$. We see that the formal analysis is the same as for multicomponent signals.

The STFT for the sampled signal (3) is of the form

$$\text{STFT}(\vec{n}_T,\vec{\omega}) = x(\vec{n}_T)\sum_{R^k} W[(\vec{\omega}+\vec{\omega}_{pk}-\nabla\Phi(\vec{r})_{|\vec{r}=\vec{n}_T}] \quad (28)$$

where we have neglected the distortions due to higher-order partial derivatives of the phase function, i.e, $\nabla\Phi(\vec{r}) = \text{const}$, and $\vec{n}_T = (n_1T_1, n_2T_2, \cdots, n_nT_n)$.

Combining the previous relation with (17), the PWD of discretized signal is obtained

$$\text{PWD}(\vec{n}_T,\vec{\omega}) = \sum_{R^{k_1}}\sum_{R^{k_2}}\frac{|g(\vec{n}_T)|^2}{\pi^n} \times \int_{R^n} W[\vec{\omega}+\vec{\theta}+\vec{\omega}_{pk_1}-\nabla\Phi(\vec{r})_{|\vec{r}=\vec{n}_T}] \times W^*[\vec{\omega}-\vec{\theta}+\vec{\omega}_{pk_2}-\nabla\Phi(\vec{r})_{\vec{r}=\vec{n}_T}]\,dV_{\vec{\theta}}. \quad (29)$$

Using similar procedure as in the cross-terms analysis, it may be seen that the integrand is nonzero if the following holds

$$-W_h/2-(k_{1h}-k_{2h})\omega_{ph}/2 < \theta_h < W_h/2-(k_{1h}-k_{2h})\omega_{ph}/2, \quad h = 1, 2, \cdots, n \quad (30)$$

where W_h is the width of $W(\vec{x})$ in the ω_h direction. It is obvious that the auto-terms ($k_{1h} = k_{2h}$) appear due to the integration around the $\vec{\theta}$ origin. The closest aliasing components along θ_h axis are those for $k_{1h} - k_{2h} = \pm 1$. Obviously, they may be eliminated by using a window $P(\vec{\theta})$, equal to zero along the θ_h axis, for the values of θ_h outside the interval $|\theta_h| < \omega_{ph}/2 - W_h/2$. Observe that this condition is usually significantly relaxed, as compared to the condition for eliminating cross-terms, Fig. 2. Thus, the window $P(\vec{\theta})$ satisfying the previous conditions guarantees the elimination of the aliasing components, i.e., the oversampling is not necessary.

VI. Numerical Considerations for Two-Dimensional Case

We will compare the modified WD with the conventional PWD, with respect to the number of operations needed for their respective numerical computations. To simplify the presentation, we will consider the two-dimensional case, which is presently the only one of practical interest.

The discrete two-dimensional PWD is of the form

$$\begin{aligned}&\mathrm{WD}(n_1, n_2, k_1, k_2)\\ &= 4\sum_{m_1=0}^{2N-1}\sum_{m_2=0}^{2N-1} x(n_1+m_1, n_2+m_2)x^*(n_1-m_1, n_2-m_2)\\ &\qquad\cdot \times e^{-j\frac{4\pi}{2N}(k_1 m_1 - k_2 m_2)}\end{aligned} \tag{31}$$

where N is the number of samples, determined according the sampling theorem.

The modified WD (21), may be expressed in the discrete form for a rectangular window $P_d(i_1, i_2)$, as

$$\begin{aligned}&\mathrm{MWD}(n_1, n_2, k_1, k_2)\\ &= |\mathrm{STFT}(n_1, n_2, k_1, k_2)|^2\\ &\quad + 2\sum_{i_1=0}^{L}\sum_{i_2=1}^{L} \mathrm{Real}\{\mathrm{STFT}(n_1, n_2, k_1+i_1, k_2+i_2)\\ &\qquad\qquad \times \mathrm{STFT}^*(n_1, n_2, k_1-i_1, k_2-i_2)\}\\ &\quad + 2\sum_{i_1=1}^{L}\sum_{i_2=-L}^{0} \mathrm{Real}\{\mathrm{STFT}(n_1, n_2, k_1+i_1, k_2+i_2)\\ &\qquad\qquad \times \mathrm{STFT}^*(n_1, n_2, k_1-i_1, k_2-i_2)\}\end{aligned} \tag{32}$$

with $L_1 = L_2 = L$. where $2L_1 + 1$ and $2L_2 + 1$ represent the widths of two-dimensional window $P_d(i_1, i_2)$. Sampling in the STFT is defined by sampling theorem, and so is in the modified WD due to $P_d(i_1, i_2)$.

The computation time may be reduced using an iterative procedure for computation of the STFT

$$\begin{aligned}&\mathrm{STFT}(n_1, n_2+1, k_1, k_2)\\ &\quad = \{\mathrm{STFT}(n_1, n_2, k_1, k_2) + \mathcal{F}_{n_1}[x(n_1, n_2+N)]\\ &\qquad - \mathcal{F}_{n_1}[x(n_1, n_2)]\}e^{j\frac{2\pi}{N}k_2}\\ &\mathrm{STFT}(n_1+1, n_2, k_1, k_2)\\ &\quad = \{\mathrm{STFT}(n_1, n_2, k_1, k_2) + \mathcal{F}_{n_2}[x(n_1+N, n_2)]\\ &\qquad - \mathcal{F}_{n_2}[x(n_1, n_2)]\}e^{j\frac{2\pi}{N}k_1}\end{aligned} \tag{33}$$

where $\mathcal{F}_{n_m}$ is one-dimensional STFT over n_m, and the window $w(\vec{n})$ is shaped as a rectangle.

Numbers of numeric operations required for the direct realization of the PWD defined by (31) (using the FFT routines), as well the numbers for the modified WD, (32), are given in Table I.

Let us compare the number of multiplications needed for the computation of (31) with that in (32), taking into account (33).

TABLE I
The Numbers of Complex Operations Required for the Realization of Wigner Distribution and Modified Wigner Distribution

Method	Complex additions	Complex multiplications
Direct WD calculation	$4N^2(\log_2 N+1)$	$2N^2(\log_2 N+2)$
Proposed method	$N^2(2\log_2 N+L^2+L)$	$N^2(\log_2 N+L^2+L+1/2)$
Proposed method using recursive STFT realization	$N^2(L^2+L+2)$	$N^2(L^2+L+3/2)$

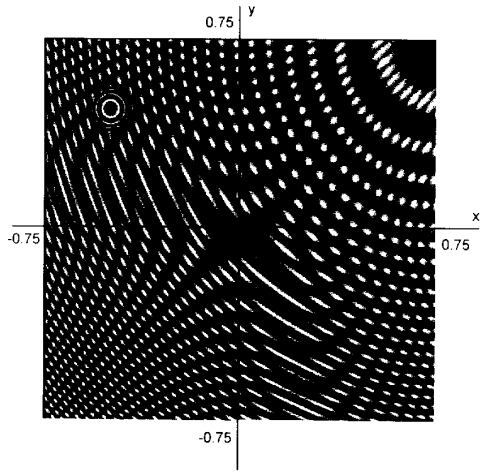

Fig. 3. Two-dimensional signal.

The savings by the proposed method are achieved if the following inequality holds

$$2(\log_2 N + 2) > (L^2 + L + 3/2). \tag{34}$$

To illustrate this point, take, for example, $N = 64$. The savings in the number of computations are achieved if $L \leq 3$. i.e., the width of the window $P_d(i_1, i_2)$ is less or equal to 7×7. Superiority of the proposed method is even more evident if we consider the required number of additions.

VII. Numerical Example

To illustrate the proposed method, consider the two-dimensional signal

$$\begin{aligned}f(x, y) &= \cos[20\pi(x-0.75)^2 + 22\pi(y-0.75)^2]\\ &\quad + 0.5e^{j[(-100\cos(\pi x/2) - 100\cos(\pi y/2))]}\end{aligned}$$

in the range:$|x| < 0.75$, $|y| < 0.75$. This signal belongs to the class (13). Fig. 3 shows its real part, combined with the signal

$$f_s(x, y) = \cos\{1000\pi[(x+0.5)^2 + (y-0.5)^2]\}$$

whose domain: $|x + y| < 0.1$, $|y - x - 1| < 0.1$, is comparatively small, i.e., its Fourier transform may be treated as the one described by (22).

We have applied the Hanning window whose widths along x and y axes are $W_x = W_y = 1$. For the computation of the STFT we have taken $N = 64$ samples, while the corresponding number for the computation of the PWD is $M = 2N = 128$ samples. The STFT, the PWD and modified WD are computed at the point $(x, y) = (-0.25, -0.25)$, and the results are presented in Fig. 4.

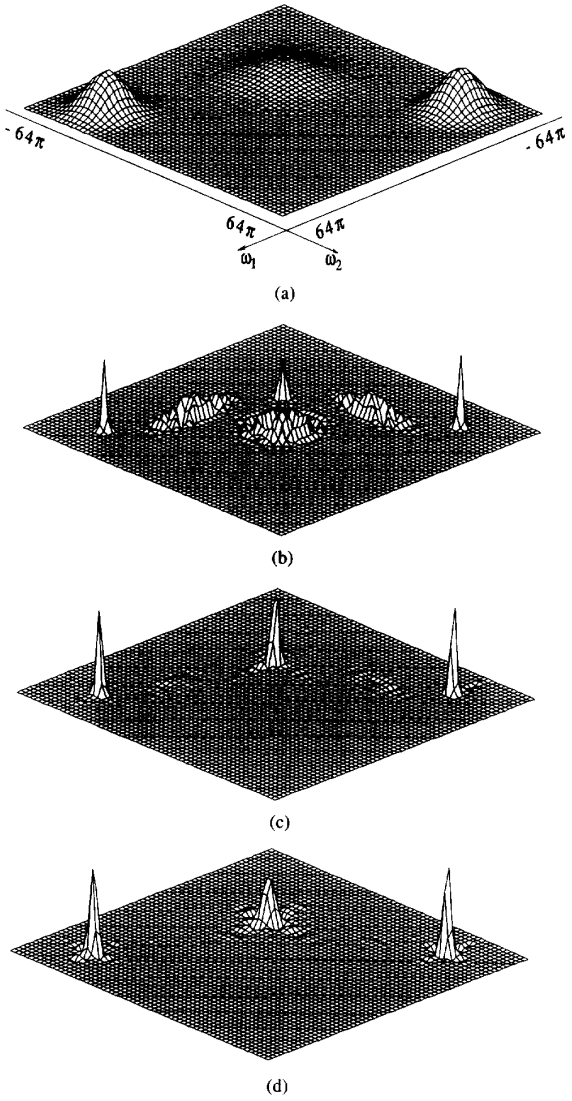

Fig. 4. Local frequency representation of a two-dimensional signal: a) spectrogram, b) Wigner distribution, c) modified Wigner distribution $L = 8$, and d) modified Wigner distribution $L = 3$.

VIII. Conclusion

Comparison of the commonly used multidimensional time-frequency distributions with the distribution which ideally represents the local frequency or group shift is presented. A numerically efficient method for cross-terms reduction or removal in the Wigner distribution is proposed.

The multidimensional time-frequency signal analysis may be useful in many complex practical and theoretical problems. From the numerical example it is obvious that one instance where these distributions may be used is the local frequency image analysis. Recently, the electromagnetic field, scattered or diffracted from the finite structures, has been analyzed using the one-dimensional time-frequency (space-wave number) distributions [15]. These distributions are suitable only when the structure is finite in one dimension. However, if the structure is finite in more than one direction (finite grating strip, open waveguide, . . .) then the need for multidimensional time-frequency analysis is apparent. Also, if a one-dimensional signal propagates through a nonhomogenious media, then the variation along the direction of propagation is equally important as the time variation of spectral components. In this case, for a complete analysis, the signal should be known over both time and space. Thus, one can make conclusions not only about the signal but also about the media of propagation, which in some cases may be the primary research issue.

Multidimensional approach to the physical problems provides deeper insight into the nature of a process, as well as the possibility of taking into account the more complex forms. But, it also requires very complex multidimensional mathematical techniques. One of them is the multidimensional time-frequency analysis, which may gain importance with further development of computer hardware and software.

References

[1] L. Cohen, "Time-frequency distributions—A review," *Proc. IEEE*, vol. 77, pp. 941–981, July 1989.

[2] Y. M. Zhu, F. Peyrin, and R. et Goutte, "Transformation de Wigner-Ville: Description d'un nouvel outil de traitement du signal et des images," *Annales Des Telecomm.*, vol. 42, no. 3–4, pp. 105–117, 1987.

[3] S. Kadambe and G. F. Boudreaux-Bartels, "A comparison of the existence of cross terms in the Wigner distribution and squared magnitude of the wavelet transform and short time Fourier transform," *IEEE Trans. Signal Processing*, vol. 40, no. 10, pp. 2498–2517, Oct. 1992.

[4] LJ. Stanković, "A method for time-frequency analysis," *IEEE Trans. on SP*, vol. 42. no. 1, Jan. 1994.

[5] LJ. Stanković and S. Stanković, "An analysis of instantaneous frequency representation using time-frequency distributions—generalized Wigner distribution," *IEEE Trans. Signal Processing*, vol. 43, no. 2, pp. 549–552, Feb. 1995.

[6] LJ. Stanković, "A method for improved energy concentration in the time-frequency analysis of multicomponent signals using the L-Wigner distribution," *IEEE Trans. Signal Processing*, scheduled May 1995.

[7] ——, "An analysis of some time-frequency and time scale distributions," *Ann. Telecommun.*, no. 9–10, pp. 505–517, Sept./Oct. 1994.

[8] ——, "Multitime definition of the Wigner higher order distribution: L-Wigner distribution," *IEEE Signal Processing Lett.*, no. 7, pp. 106–109, July 1994.

[9] ——, "Auto term representation by the reduced interference distributions; the procedure for a kernel design," *IEEE Trans. Signal Processing*, submitted.

[10] D. E. Dudgeon and R. M. Mersereau, *Multidimensional Digital Signal Processing*. Englewood Cliffs, NJ: Prentice Hall, 1984.

[11] L. Cohen, "Distribution concentrated along the instantaneous frequency," *SPIE*, vol. 1348, *Advanced Signal Processing Algorithms, Architecture, and Implementation*, pp. 149–157, 1990.

[12] H. I. Choi and W. J. Williams, "Improved time-frequency representation of multi-component signals using exponential kernels," *IEEE Trans. Acoust., Speech, Signal Processing*, vol. 37, no. 6, pp. 862–871, June 1989.

[13] Y. Zhao, L. E. Atlas, and R. J. Marks II, "The use of cone-shaped kernels for generalized time-frequency representation for nonstationary signals," *IEEE Trans. Acoust., Speech, Signal Processing*, vol. 38, no. 7, pp. 1084–1091, July 1990.

[14] A. H. Costa and G. F. Boudreaux-Bartels, "A comparative study of alias-free time frequency representations," in *Proc. of the IEEE-SP Int. Symp. TFTSA*, Philadelphia, PA, Oct. 1994, pp. 72–75.

[15] L. Carin and L. B. Felsen, "Wave oriented data processing for frequency and time domain scattering by nonuniform truncated arrays," *IEEE Antennas and Propagation Mag.*, no. 3, pp. 29–43, June 1994.

[16] J. Jeong and W. J. Williams, "Kernel design for reduced interference distributions," *IEEE Trans. Signal Processing*, no. 2, pp. 402–412, Feb. 1992.